

FoxOs Are Lineage-Restricted Redundant Tumor Suppressors and Regulate Endothelial Cell Homeostasis

Ji-Hye Paik,^{1,2,11} Ramya Kolipara,^{1,2,11} Gerald Chu,^{1,2,4,5} Hongkai Ji,⁶ Yonghong Xiao,⁵ Zhihu Ding,^{1,2} Lili Miao,^{1,2,5} Zuzana Tothova,⁷ James W. Horner,^{1,2,3} Daniel R. Carrasco,^{1,2,3,4,5} Shan Jiang,^{1,2} D. Gary Gilliland,⁷ Lynda Chin,^{1,2,5,8} Wing H. Wong,⁹ Diego H. Castrillon,^{1,4,10,*} and Ronald A. DePinho^{1,2,3,5,*}

¹Department of Medical Oncology, Dana-Farber Cancer Institute

²Department of Medicine

³Department of Genetics

⁴Department of Pathology, Brigham and Women's Hospital

⁵Center for Applied Cancer Science, Belfer Foundation Institute for Innovative Cancer Science, Dana-Farber Cancer Institute Harvard Medical School, Boston, MA 02115, USA

⁶Department of Statistics, Harvard University, Cambridge, MA 02138, USA

⁷Division of Hematology, Department of Medicine, Brigham and Women's Hospital, Boston, MA 02115, USA

⁸Department of Dermatology, Harvard Medical School, Boston, MA 02115, USA

⁹Department of Statistics, Stanford University, Stanford, CA 94305, USA

¹⁰Department of Pathology and Simmons Comprehensive Cancer Center, University of Texas Southwestern Medical School, Dallas, TX 75390, USA

¹¹These authors contributed equally to this work.

*Correspondence: diego.castrillon@utsouthwestern.edu (D.H.C.), ron_depinho@dfci.harvard.edu (R.A.D.)

DOI 10.1016/j.cell.2006.12.029

SUMMARY

Activated phosphoinositide 3-kinase (PI3K)-AKT signaling appears to be an obligate event in the development of cancer. The highly related members of the mammalian FoxO transcription factor family, FoxO1, FoxO3, and FoxO4, represent one of several effector arms of PI3K-AKT signaling, prompting genetic analysis of the role of FoxOs in the neoplastic phenotypes linked to PI3K-AKT activation. While germline or somatic deletion of up to five FoxO alleles produced remarkably modest neoplastic phenotypes, broad somatic deletion of all FoxOs engendered a progressive cancer-prone condition characterized by thymic lymphomas and hemangiomas, demonstrating that the mammalian FoxOs are indeed bona fide tumor suppressors. Transcriptome and promoter analyses of differentially affected endothelium identified direct FoxO targets and revealed that FoxO regulation of these targets in vivo is highly context-specific, even in the same cell type. Functional studies validated Sprouty2 and PBX1, among others, as FoxO-regulated mediators of endothelial cell morphogenesis and vascular homeostasis.

INTRODUCTION

The PI3K-AKT pathway is activated in human cancers, commonly through genetic alterations of its many signaling components. AKT and the p110 α catalytic subunit of PI3K is mutated or amplified and overexpressed in several cancer types, and PTEN, the key PI3K-AKT pathway antagonist, is also inactivated in a broad spectrum of human cancers (Cully et al., 2006). Moreover, germline PTEN mutations define three related syndromes characterized by hamartomas, cancer, and developmental defects (Wanner et al., 2001). PTEN's diverse tumor suppressor role in different cell lineages is further evidenced by the cancer-prone condition in germline and conditional *Pten* mutant mice, which develop carcinomas of the skin, prostate, colon, breast, and endometrium, as well as thymic lymphomas, among other cancers (Di Cristofano et al., 1998; Li et al., 2002; Podsypanina et al., 1999; Suzuki et al., 2001; Wang et al., 2003; You et al., 2002). In addition to a direct role in tumor development, PI3K-AKT signaling has been linked to endothelial cell (EC) homeostasis (Shiojima and Walsh, 2002). One of the PTEN germline mutation syndromes, Bannayan-Zonana, is characterized by hemangiomas (EC hamartomas) in diverse tissues (Wanner et al., 2001), and *Pten* heterozygous mice develop hemangiomas with high penetrance (Freeman et al., 2006).

The wide range of benign to malignant phenotypes mediated by PI3K-PTEN-AKT signaling is consistent with the existence of diverse downstream effectors differentially

utilized in conferring neoplastic phenotypes in distinct cell lineages. Among such potential effectors are AKT phosphorylation targets TSC2, GSK3, and the FoxOs (Brunet et al., 1999; Cross et al., 1995; Inoki et al., 2002). Recently, much attention has been focused on TSC2 and mTOR signaling as mounting pharmacological evidence suggests that mTOR is the prime effector of the PI3K-AKT pathway, with TSC2 serving as a central node linking LKB1-AMPK and PI3K-AKT with mTOR (Hay, 2005). Indeed, the potent anti-neoplastic impact of pharmacologic mTOR inhibition raises questions as to the relevance of other AKT targets, particularly the FoxOs, in the development of cancer. On the other hand, the FoxO effector arm controls cell number in *Drosophila* (Junger et al., 2003; Puig et al., 2003), and the FoxO transcription factors mediate some of the growth and survival-promoting effects of AKT signaling in ECs (Potente et al., 2005; Skurk et al., 2004). Therefore, the relevance of FoxO transcription factors in cancer and their roles in normal tissue homeostasis remain to be elucidated.

Whereas *C. elegans* and *Drosophila* contain a single FoxO gene (DAF-16 and dFOXO, respectively), mice and humans possess three highly related FoxO homologs (FoxO1, FoxO3, and FoxO4) with overlapping patterns of expression and transcriptional activities (Anderson et al., 1998; Biggs et al., 2001; Furuyama et al., 2000). A fourth more distantly related mammalian FoxO family member, FoxO6, has been identified, although it appears to be regulated by distinct mechanisms and its expression is more highly restricted to the brain (Jacobs et al., 2003; van der Heide et al., 2005).

In cell culture-based systems, FoxO1, FoxO3, and FoxO4 behave similarly in biochemical studies, appear to regulate common target genes, and bind to the same target DNA sequence (Biggs et al., 2001; Brunet et al., 1999; Furuyama et al., 2000). Yet, mouse FoxO knockouts have revealed unique roles for the FoxOs, such as the requirement for FoxO3 in ovarian primordial follicle activation (Castrillon et al., 2003; Hosaka et al., 2004) and FoxO1 in vasculogenesis (Furuyama et al., 2004; Hosaka et al., 2004). However, while the three FoxOs serve some discrete functions, they likely have significant redundancies, as they are broadly expressed during embryonic development and in adult tissues (Furuyama et al., 2000). In this regard, conventional genetic analysis can fail to uncover important biological functions among closely-related gene families, such as Rb/p107/p130 (Lee et al., 1996; Sage et al., 2000) and p53/p63/p73 (Flores et al., 2002; 2005). Indeed, many analogies can be drawn between the FoxO, Rb, and p53 gene families, all of which regulate cell survival and growth and consist of members with common physiological roles.

In the context of the linkage of FoxOs to key cancer signaling pathways, the lack of an overt tumor-prone phenotype of the various FoxO knockout mice was somewhat unanticipated (Castrillon et al., 2003; Hosaka et al., 2004; Lin et al., 2004). While this may relate to the physical and functional relatedness and overlapping expression

patterns of the FoxO members, it is formally possible that the FoxO arm of the PI3K-AKT signaling network plays a relatively minor in vivo role in cancer suppression and vascular biology relative to other AKT downstream targets. To address these issues, we have generated conditional alleles for all three FoxO members with which to conduct a systematic evaluation of FoxO family function in vivo.

RESULTS

Somatic Deletion of All Three FoxO Genes Results in Lineage-Restricted Tumor Phenotypes

To genetically assess the cancer relevance of the FoxO members in vivo, we generated null and conditional alleles for all three FoxO genes (see the Supplemental Data text and Figures S1 and S2). Exhaustive characterization of mice bearing single and compound germline FoxO null mutations, including FoxO1^{-/-};FoxO3^{-/-};FoxO4^{-/-} mice, revealed remarkably mild cancer predisposition phenotypes as a function of advancing age or following carcinogen treatment (Figures S3–S6, and see Table S1 in the Supplemental Data). The potential for redundancy and developmental compensation among the FoxOs, coupled with the embryonic lethality of FoxO1 deficiency (Furuyama et al., 2004; Hosaka et al., 2004), prompted the use of the inducible Mx-Cre transgene to achieve widespread somatic FoxO deletion in adult tissues. The Mx1 promoter is activated by polyinosine-polycytidylic acid (pl-pC), and pl-pC injection at 4–5 weeks of age results in transient widespread Cre expression (Kuhn et al., 1995) (see Mx1 promoter-directed tissue distribution of Cre below).

To delete the FoxO genes in vivo, Mx-Cre⁺;FoxO1/3/4^{L/L} and control littermate Mx-Cre⁻;FoxO1/3/4^{L/L} mice (hereafter designated as “Mx-Cre⁺” and “Mx-Cre⁻,” respectively) were injected with pl-pC. By 19–30 weeks of age, Mx-Cre⁺ mice developed aggressive CD4⁺ CD8⁺ lymphoblastic thymic lymphomas, with spread to spleen, liver, and lymph nodes (Figures 1A, 1B, and 1F, $p < 0.0001$). While Mx-Cre-mediated gene deletion in the thymus was incomplete (Kuhn et al., 1995) (Figure 1C), the lymphomas display an enrichment of the null alleles for all three FoxO genes (Figure 1C) accompanied by a marked decrease of FoxO expression on both mRNA and protein levels (Figures 1D and 1E). This and the lack of lymphomas in all other genotypes retaining at least one FoxO allele (Figure 1A) is consistent with the need for complete FoxO deficiency in lymphomagenesis.

In addition, all Mx-Cre⁺ mice developed a striking age-progressive hamartomatous phenotype in the EC lineage, with widespread hemangiomas, resulting in premature death (Figure 2A). Hemangiomas were most exaggerated in the uterus and evident by 6–8 weeks, but greatly progressed by 30–40 weeks (Figure 2B). Histological examination revealed massive hemangiomas with intraluminal blood and thrombi in skeletal muscle, abdominal wall, liver, adrenal glands, bone marrow, omentum, lymph node, and skin (Figure 2C; Figure S7A). The ECs in most

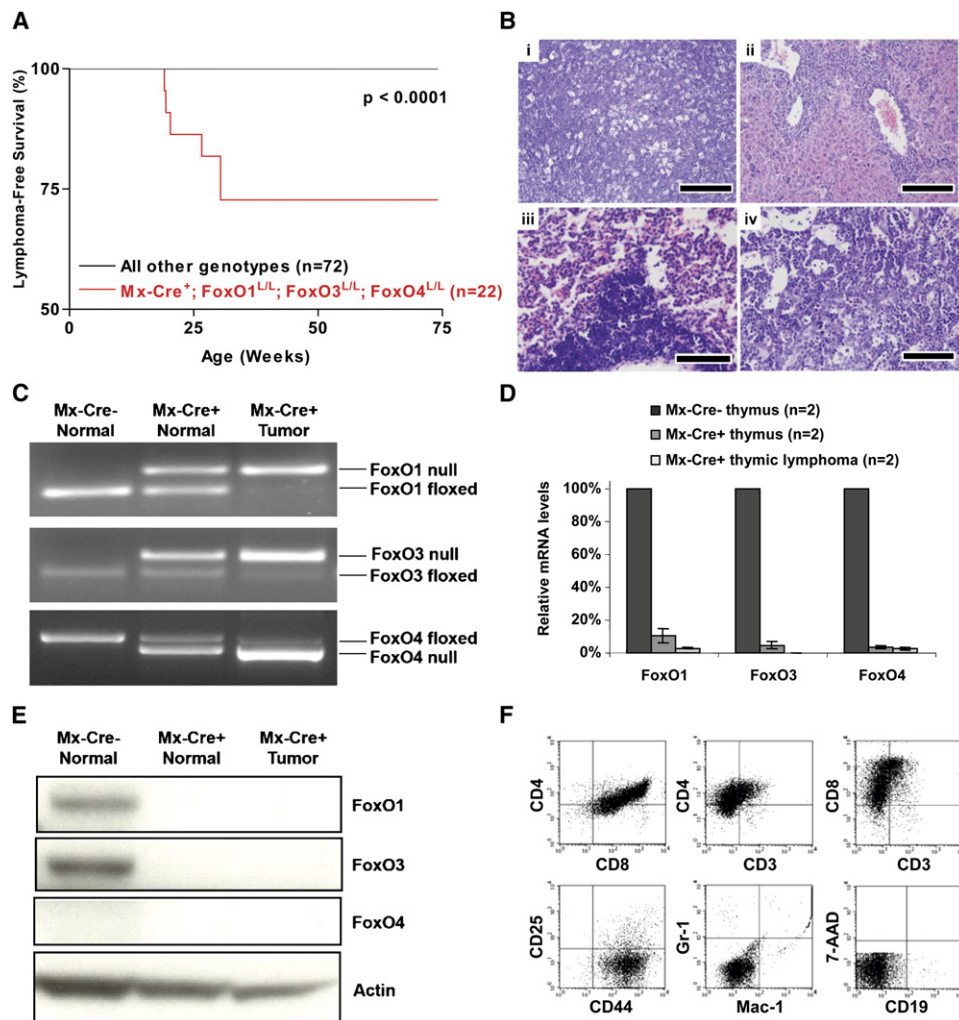


Figure 1. Thymic Lymphomas in Mice Following Somatic Deletion of Three *FoxO* Genes

(A) Thymic lymphoma-free survival of pl-pC-treated *Mx-Cre*⁺ mice and controls representing combined genotypes including *Mx-Cre*⁺;*FoxO1*^{L/L} (n = 11), *Mx-Cre*⁺;*FoxO1/3*^{L/L} (n = 14), *Mx-Cre*⁺;*FoxO1/4*^{L/L} (n = 11), and all *Mx-Cre*⁻ controls (n = 36). No lymphomas were observed in controls up to 100 weeks of age.

(B) Histology and tissue infiltration of thymic lymphoma in *Mx-Cre*⁺ mouse, H&E stains. i, thymus; ii, liver, iii, lung; and iv, bone marrow. Scale bars, 200 μm (i and ii) and 100 μm (iii and iv).

(C) *FoxO1*, *FoxO3*, and *FoxO4* gene deletions in thymic lymphomas and control thymi by PCR analysis.

(D) Reduction of mRNA levels of *FoxO1*, *FoxO3*, and *FoxO4* in *Mx-Cre*⁺ ECs. Quantitative RT-PCR performed on *Mx-Cre*⁻ thymi (7 weeks), *Mx-Cre*⁺ thymi (7 weeks), and *Mx-Cre*⁺ thymic lymphomas (n = 2, 19, and 30 weeks post pl-pC); relative reduction of *FoxO* levels relative to *Mx-Cre*⁻ thymi is shown. Error bars represent ±SE.

(E) Western blot analysis of *Mx-Cre*⁻ and *Mx-Cre*⁺ thymi and thymic lymphoma samples.

(F) Flow cytometric analysis of representative thymic lymphoma.

lesions appeared benign; however, 9% of *Mx-Cre*⁺ mice progressed to lethal angiosarcomas (Figure 2C).

Labeling of ECs with fluorescein-conjugated lectin revealed significant increases in the numbers of ECs in affected organs (Figure 2D). This proliferative phenotype was apparent as early as 3 weeks after pl-pC injection, prior to onset of macroscopic abnormalities in these vascular beds. In contrast, ECs in the lung and kidney (where hemangiomas do not develop following documented *FoxO* deletion) did not show any abnormalities, even at

27 weeks after pl-pC injection, establishing tissue-context requirements for the *FoxOs* in vivo across this single lineage (Figure 2D).

Further support for a role of the *FoxOs* in this vascular phenotype stems from observations of less severe hemangiomas in *Mx-Cre*⁺ mice with a deficiency of only one or two *FoxO* genes. By 60 weeks of age, 100% of *Mx-Cre*⁺;*FoxO1*^{L/L} females displayed mild hemangiomas in the uterus and occasionally in perirenal fat, with no abnormalities in other tissues (Figure S7B). *Mx-Cre*⁺;*FoxO1/4*^{L/L}

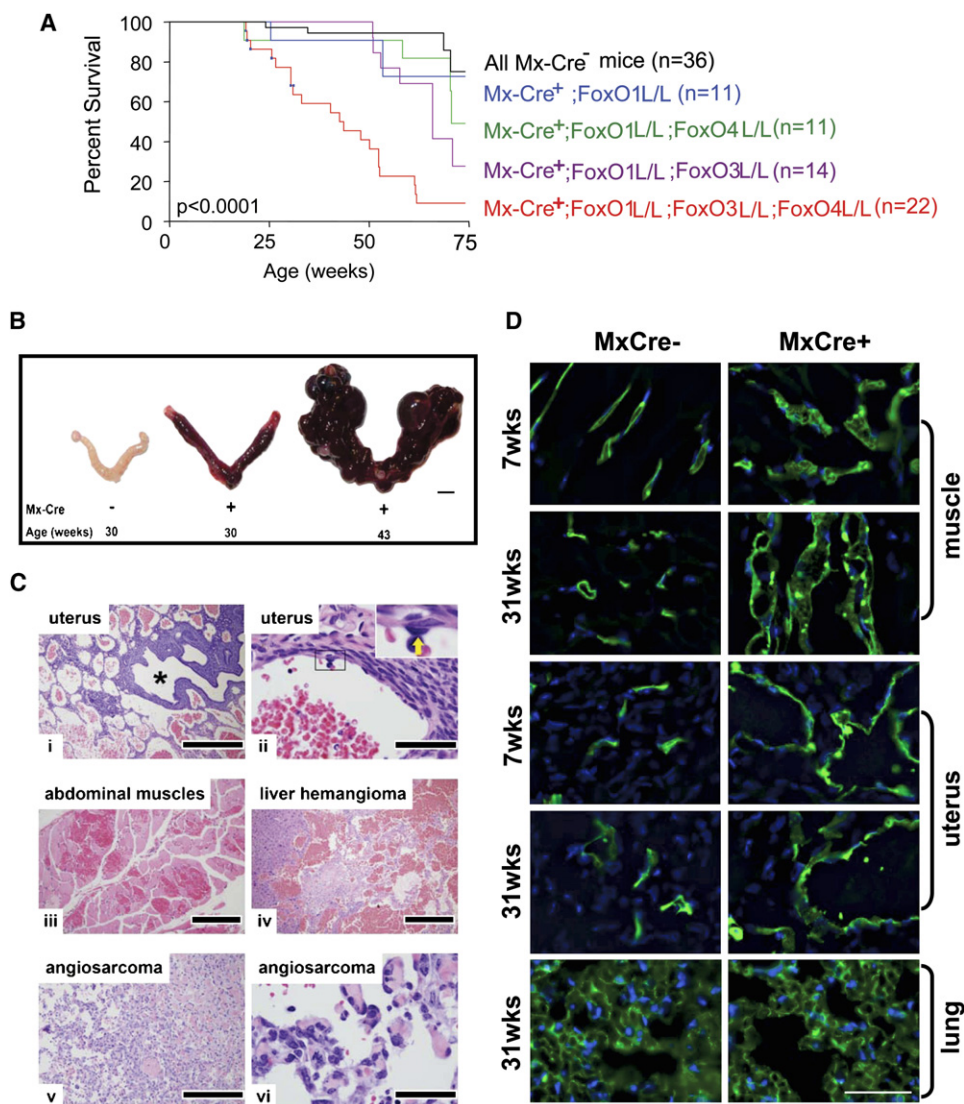


Figure 2. Systemic Hemangiomas in Mice Following Somatic Deletion of Three *FoxO* Alleles

(A) Survival of *Mx-Cre*⁺ and *Mx-Cre*⁻ littermate controls. Small blue squares indicate deaths due to thymic lymphomas. *p* value indicates comparison between *Mx-Cre*⁺ mice (red) and all *Mx-Cre*⁻ controls (black).

(B) Age-dependent progression of uterine vascular lesions in *Mx-Cre*⁺ females. Scale bar, 5 mm.

(C) Histology of systemic vascular lesions, H&E stains. Genotypes are *Mx-Cre*⁺ unless otherwise noted. i, uterus, low magnification (asterisk: uterine lumen); ii, uterine hemangioma (inset: benign endothelium of hemangioma vascular channels; arrow: endothelial cell); iii, abdominal muscle hemangioma; iv, liver hemangioma, *Mx-Cre*⁺ mouse; v–vi, angiosarcoma, *Mx-Cre*⁺ mouse. Scale bars, 500 μ m (i and v), 400 μ m (iv), 200 μ m (iii), and 50 μ m (ii and vi).

(D) Fluorescence micrographs of abdominal muscle, uterine horn, and lung endothelium after vascular perfusion of fluorescein-labeled lectin (blue: DAPI-labeled nuclei). Note increased EC density by 7 weeks in muscle and uterine horn, but not in lung, as late as 31 weeks. Scale bar, 50 μ m.

mice also displayed mild hemangiomas in the uterus and occasionally in other tissues (Figure S7C), and all *Mx-Cre*⁺; *FoxO1*^{3^{L/L}} mice displayed vascular abnormalities with similar tissue distribution as *Mx-Cre*⁺; *FoxO1*^{3/4^{L/L}} mice (Figure S7D). Importantly, these hemangiomatous lesions that retained either *FoxO3* or *FoxO4* were significantly less severe as reflected by lack of mortality prior to 50 weeks of age (Figure 2A). In contrast, vascular abnormalities were not detected in *Mx-Cre*⁺; *FoxO3*^{L/L} mice

up to 21 weeks, germline *FoxO3*^{-/-}; *FoxO4*^{-/-} mice up to 2 years of age, and *FoxO1*^{-/-}; *FoxO3*^{-/-}; *FoxO4*^{-/-} mice up to 40 weeks of age. These genotype-phenotype correlations point to *FoxO1* as the most potent regulator of adult vascular homeostasis, with lesser but physiologically important contributions from the other *FoxOs*. In summary, vascular lesions were much more pervasive and severe following elimination of all three *FoxOs*, and premature mortality attributable to these vascular lesions

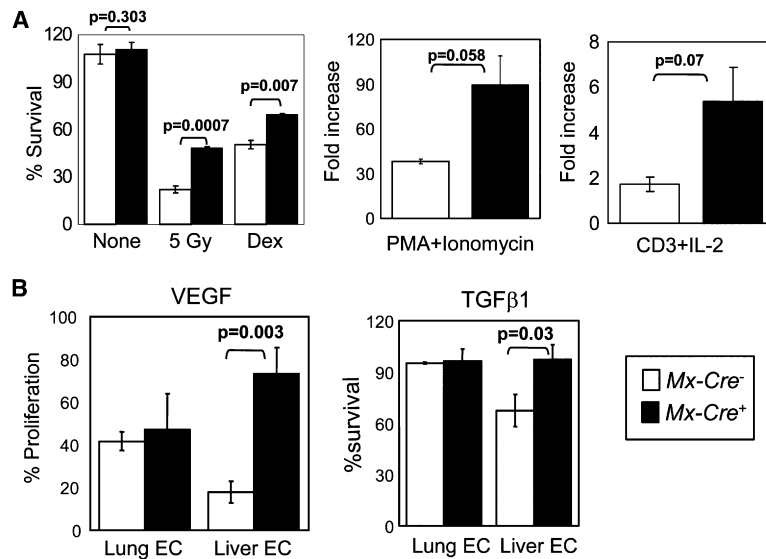


Figure 3. Functional Studies of Thymocytes and Endothelial Cells Rendered Null for All Three FoxOs

(A) Increased proliferation and defective induction of apoptosis in *Mx-Cre*⁺ thymocytes. Thymocytes from 8-week-old mice ($n = 3$ per genotype) were plated and the indicated mitogens or apoptotic stimuli were applied. The experiment was performed twice with similar results; data from a representative experiment are shown. Survival percentage was calculated after 18 hr of treatment (5 Gy: γ -irradiation; Dex: 1 μ M Dexamethasone). Data are mean \pm SEM. (B) Analysis of viability of ECs. MTT assays were performed on *Mx-Cre*⁻ and *Mx-Cre*⁺ lung ($n = 2$) and liver ($n = 3$) ECs. y axis, normalized response (%) per OD595. Results represent two independent experiments. Data are mean \pm SEM.

was observed only in mice with somatic deletion of all three FoxOs (Figure 2A).

Cell Biological Impact of FoxO Family Deletion

To understand how the FoxOs constrain the development of thymic lymphoma and hemangiomas, we examined the proliferative and survival profiles of thymocyte and ECs derived from young cancer-free mice. Although histologically normal (data not shown), albeit with a slight reduction in total number of thymocytes compared to *Mx-Cre*⁻ controls ($99,110,000 \pm 13,590,000$ versus $147,300,000 \pm 20,950,000$; $n = 6$ each; $p = 0.0825$), *Mx-Cre*⁺ thymocytes exhibited altered responses to growth and death stimuli. Upon stimulation with PMA + ionomycin, *Mx-Cre*⁺ thymocytes showed increased proliferation relative to *Mx-Cre*⁻ controls (Figure 3A). Proliferative enhancement was also observed with CD3 + IL2 stimulation (Figure 3A). Conversely, *Mx-Cre*⁺ thymocytes were more resistant to cell death stimuli such as γ -irradiation and high-dose dexamethasone treatment (Figure 3A). These observations indicate that complete loss of FoxO gene function in thymocytes predisposes to lymphomagenesis through cell-autonomous mechanisms that enhance cellular proliferation and survival.

Taking advantage of efficient *Mx-Cre*-mediated recombination in ECs in all tissue compartments examined (Figure S8) (Hayashi et al., 2004; Schneider et al., 2003) and the organ-restricted hemangioma phenotype in *Mx-Cre*⁺ mice, we compared the biological consequences of complete FoxO deletion in ECs from affected and unaffected vascular beds in different tissues. ECs were isolated and cultured from lung (which displayed no phenotype in vivo) and liver (which displayed prominent hemangiomatic changes) from age-matched mice. The purity of these cell preparations was >97% by flow cytometry for CD31 and immunostaining for VE-cadherin and CD31 (Figures S9A and S9B). Efficient deletion of all three FoxO alleles was confirmed by PCR, and western blot

documented absence of FoxO protein in both lung and liver ECs (Figures S9C and S9D). In vivo, absence of mRNA for all three FoxOs in the vasculature of lung, liver, and uterus was documented by RNA in situ hybridization (RISH) (Figure S10).

Relative to *Mx-Cre*⁺ lung ECs, *Mx-Cre*⁺ liver ECs showed enhanced proliferative response to stimulation by VEGF and bFGF, two potent proangiogenic cytokines (Bikfalvi et al., 1997; Ferrara et al., 2003). While *Mx-Cre*⁻ and *Mx-Cre*⁺ lung ECs responded to VEGF similarly regardless of their FoxO status, *Mx-Cre*⁺ liver ECs exhibited a dramatic enhancement in their ability to proliferate upon VEGF stimulation (Figure 3B; 73% versus 17.9%, $p = 0.003$). A similar trend was observed with bFGF stimulation ($p = 0.019$; data not shown). Conversely, *Mx-Cre*⁺ liver ECs were significantly less sensitive to TGF- β 1, a cytokine that induces EC cytostasis through Smad (Goumans et al., 2003), consistent with documented direct interactions between Smad and FoxO (Seoane et al., 2004). Here, *Mx-Cre*⁻ liver ECs showed reduced survival (~60%) upon exposure to TGF- β 1, whereas *Mx-Cre*⁺ liver ECs were much less sensitive (Figure 3B). Interestingly, lung ECs were insensitive to TGF- β 1 stimulation irrespective of FoxO status (Figure 3B). In summary, mirroring the in vivo phenotypes, FoxO-deficient liver ECs exhibited enhanced proliferative and survival potential, while FoxO-deficient lung ECs did not show detectable phenotypic alterations. That FoxO exerts these biological effects in a cell-autonomous manner is supported by the observation of a prominent hemangiomatic phenotype in skeletal muscle, which showed a lack of *Mx-Cre*-mediated recombination in the surrounding skeletal muscle fibers yet efficient recombination in the endothelium (Figure S8K).

Integrated Transcriptome and Promoter Analysis Identifies Direct FoxO Targets In Vivo

The above in vivo and in vitro phenotypic characterization shows that FoxO family functions in normal tissue

homeostasis and cancer suppression are not only lineage-restricted, but also organ-specific. To gain additional insights into the mechanistic basis for such specificity, we conducted comparative transcriptome analyses of purified lung and liver ECs following pl-pC treatment of age-matched *Mx-Cre*⁺ and *Mx-Cre*[−] mice. We hypothesized that normalization against phenotypically unaffected lung ECs would provide an effective biological filter for identifying physiologically relevant FoxO targets versus secondary/bystander transcriptional events—the latter would include genes whose expression responds to FoxO regulation but who do not play a rate-limiting role in the observed phenotypes, as well as those whose expression might be altered by activation of Cre expression during FoxO deletion. Transcriptome profiles of liver ECs with and without functional FoxOs were compared with those of lung ECs (see [Experimental Procedures](#)) to generate a list of 138 significantly differentially expressed genes—89 of which were upregulated and 49 downregulated in liver, but not in lung, ECs upon documented FoxO deletion ([Table S3](#)). Consistent with the observed in vivo phenotypes, several differentially expressed genes have validated roles in EC biology, angiogenesis, and tissue morphogenesis, such as XLKD1 (LYVE-1), VCAM1, angiopoietin-like 4 (ANGPTL4), adrenomedullin (ADM), thrombospondin1 (THBS1), and ID1, and extracellular matrix proteins such as fibrillin (FBN1) (Benezra, 2001; Cook-Mills, 2002; Kato et al., 2005; Le Jan et al., 2003; Mouta Carreira et al., 2001; Ramirez et al., 1993).

Next, we reasoned that the identification of FoxO binding elements (BEs) in differentially expressed genes would provide more direct insights into FoxO's actions in the observed phenotypes. To that end, we conducted a systematic in silico analysis of the regulatory regions of these 138 genes to ascertain the presence of evolutionarily conserved FoxO consensus BEs. For each gene, the −8 kb to +2 kb region surrounding the transcription start site and the 0 to +5 kb region downstream of the transcription end site in the mouse genome was surveyed. We constructed a position-specific weight matrix (PWM) based on evolutionary conservation of canonical insulin-regulated FoxO targets (IGFBP1, G6PD, PEPCK) to characterize the FoxO binding motif (consensus = BBTRTTTDD) (D.H.C., unpublished data). Potential FoxO BEs were filtered further by cross-species conservation with two independent methodologies ([Supplemental Data](#)). BEs that could be identified in mouse, human, and at least one other species were designated as a “3-species conserved” BE. By requiring at least one evolutionary conserved FoxO BE predicted by both methods, we identified 21 putative direct targets of FoxO family in liver ECs, 9 of which were downmodulated and 12 upmodulated upon FoxO deletion ([Table 1](#)). Interestingly, several of these genes are highly relevant to cancer (e.g., TCF4), vascular biology (e.g., CTGF), or both, such as ID1 and ADM, two factors known to play critical roles in EC survival and to promote angiogenesis during development and tumori-

genesis (Benezra, 2001; Kato et al., 2005; Nikitenko et al., 2006) (see [Discussion](#)).

To validate our computational approach, we sought to document direct binding of FoxOs on predicted BEs by chromatin immunoprecipitation (ChIP) and to confirm expression modulation by quantitative RT-PCR and RISH in vitro and in vivo, respectively ([Table 1](#)). [Figure 4](#) illustrates the validation of *Sprouty2* as a direct FoxO target. First, using a mixture of anti-FoxO1/3/4 antibodies, DNA fragments spanning FoxO BEs from both the proximal and distal regions of *Sprouty2* gene were more efficiently coimmunoprecipitated in the FoxO-expressing liver ECs versus those deficient for the FoxOs ([Figure 4B](#)). Next, we documented, by immunoblotting and quantitative RT-PCR, that *Sprouty2* was significantly and reproducibly downregulated in independently derived *Mx-Cre*⁺ liver ECs, but not in *Mx-Cre*⁺ lung ECs ([Figures 4C and D](#)). Mindful of the potential artifact introduced by culturing EC in vitro, we next performed RISH in tissue sections to confirm that *Sprouty2* mRNA levels were comparable in *Mx-Cre*[−] and *Mx-Cre*⁺ lung EC but were significantly downmodulated in vascular beds of affected tissues, including liver, skeletal muscle, and uterus, in *Mx-Cre*⁺ mice 3 weeks after treatment with pl-pC ([Figure 4E](#)).

For the other targets, we conducted similar validation studies. By RISH, 12 of 14 randomly selected putative targets exhibited transcriptional regulation by FoxO in vivo ([Figure S11](#)). Of note, *Meis1* and *Klf6*, which did not confirm by RISH, were shown to be regulated by quantitative RT-PCR, pointing to the detection limits of RISH. Moreover, all 17 randomly selected putative targets (8 downmodulated and 9 upmodulated) showed expression modulation by quantitative RT-PCR in response to FoxO deletion in culture (data not shown; [Table 1](#)). Finally, all eight randomly selected putative targets (six downmodulated and two upmodulated) were validated to be true direct targets of FoxO by ChIP ([Figure S12](#)). Thus, eight of eight putative targets satisfied both ChIP and expression validation ([Table 1](#)), indicating the robustness of our integrated computational-biological approach in the identification of direct targets of FoxOs in ECs in vivo.

FoxO Activities Are Lineage-Restricted In Vivo

Next, to address whether the spectrum of downstream effectors of the FoxOs are further dictated by cell type, we performed similar in silico promoter analysis on a list of 354 most differentially expressed genes in the thymocyte lineage ([Table S2](#)) and compared these profiles with those in ECs. Strikingly, putative direct targets transcriptionally regulated by FoxOs in thymocytes with predicted FoxO BEs were completely nonoverlapping with those in EC lineage ([Table 2](#)). A notable FoxO target in thymocytes is p27^{KIP1} (*CDKN1B*), one of the downregulated genes with the highest conservation score and number of 3-species BEs (see [Discussion](#)). In other words, this in silico analysis not only identified putative targets of direct FoxO regulation, but also demonstrated in molecular terms that signaling downstream of FoxO is both cell type-specific and

Table 1. FoxO Targets in Liver EC

	FoxO Target Genes	# of BE(s)	Conservation Score	# of 3-species BE(s)	CIS	validated by RT-qPCR	validated by ChIP	validated by ISH
Downregulated FoxO Target Genes	Spry2	10	28	5		YES	YES	YES
	Tcf4	10	27	4		YES	nd	YES
	Klf6	10	28	3		YES	nd	NO
	Cited2	6	17	2		YES	YES	YES
	Adm	5	15	2		YES	YES	YES
	Ccrn4l	4	12	1		YES	YES	YES
	Hmga2	1	3	1		nd	nd	nd
	Mrc1	1	3	1		YES	YES	nd
	Ctgf	1	3	1		YES	YES	YES
Upregulated FoxO Target Genes	Meis1	10	28	4	Evi8	YES	nd	NO
	Pbx1	11	32	3		YES	YES	YES
	Tsc22d1	3	9	2		YES	nd	YES
	Ccnd1	8	25	1	Ccnd1	YES	nd	nd
	Sdpr	4	11	1		YES	nd	YES
	Sepm	4	12	1		nd	nd	nd
	Fbn1	4	12	1		YES	nd	YES
	Bmper	4	12	1		YES	YES	YES
	Rab34	3	9	1		YES	nd	nd
	D0H4S114	3	9	1		nd	nd	nd
	Pcolce	2	6	1		nd	nd	nd
	Id1	1	3	1		YES	nd	YES

YES, validated; NO, nonvalidated; nd, not determined.

tissue-specific within the same cell type. These molecular findings provide mechanistic insights and a potential explanation for the more restricted phenotypic impact of FoxO deletion relative to activated PI3K-AKT signaling in various organ systems.

Direct Effectors of FoxO-Regulated Endothelial Cell Homeostasis

To elucidate further the mechanistic basis of FoxO dysregulation in hemangioma development, we first focused on *Sprouty2* for biological validation, as it represented the most significantly regulated gene with the highest number of conserved FoxO BEs in affected liver, but not lung, EC. Using two independent *Sprouty2* shRNAs (shSpry2_1 and _2), *Sprouty2* protein knockdown of 73% to 75% was documented in primary cultures of liver ECs (Figure 5C). Passage-associated proliferative arrest of *Mx-Cre⁻* primary liver EC was reversed by *Sprouty2* knockdown, conferring enhanced replicative potential to *Mx-Cre⁻* ECs similar to that of FoxO-deficient *Mx-Cre⁺* ECs (Figure 5A). Correspondingly, increased cell cycle progression and decreased apoptosis could be demonstrated upon

Sprouty2 knockdown. Specifically, the BrdU-positive population in *Mx-Cre⁻* liver EC cultures was increased with shSpry2_1 and _2, comparable with the level of proliferation in *Mx-Cre⁺* liver ECs. Importantly, further reduction in *Sprouty2* expression in *Mx-Cre⁺* liver ECs had no additional effects (Figure 5B). Similarly, TUNEL positivity in *Mx-Cre⁻* liver ECs decreased from 19% to 7% ($p < 0.01$), comparable with the reduction to 5% observed in *Mx-Cre⁺* liver ECs ($p < 0.01$). Associated with these phenotypic changes were differential expression of CyclinD1, p15, and p21 as well as Bim following *Sprouty2* knockdown by shRNA (Figure 5D), reinforcing the view that *Sprouty2* functions as a negative regulator of EC proliferation and survival. Finally, in matrigel morphogenesis assays, *Mx-Cre⁺* liver ECs developed a more robust tube network compared with *Mx-Cre⁻* liver ECs (Figure 5E). Again, knockdown of *Sprouty2* in *Mx-Cre⁻* liver ECs enhanced such VEGF-induced tube formation to levels approaching those of *Mx-Cre⁺* liver ECs (Figure 5E). Taken together, these results demonstrate that *Sprouty2* plays essential roles in EC growth and tube morphogenesis and is a major effector of FoxO function in the endothelium.

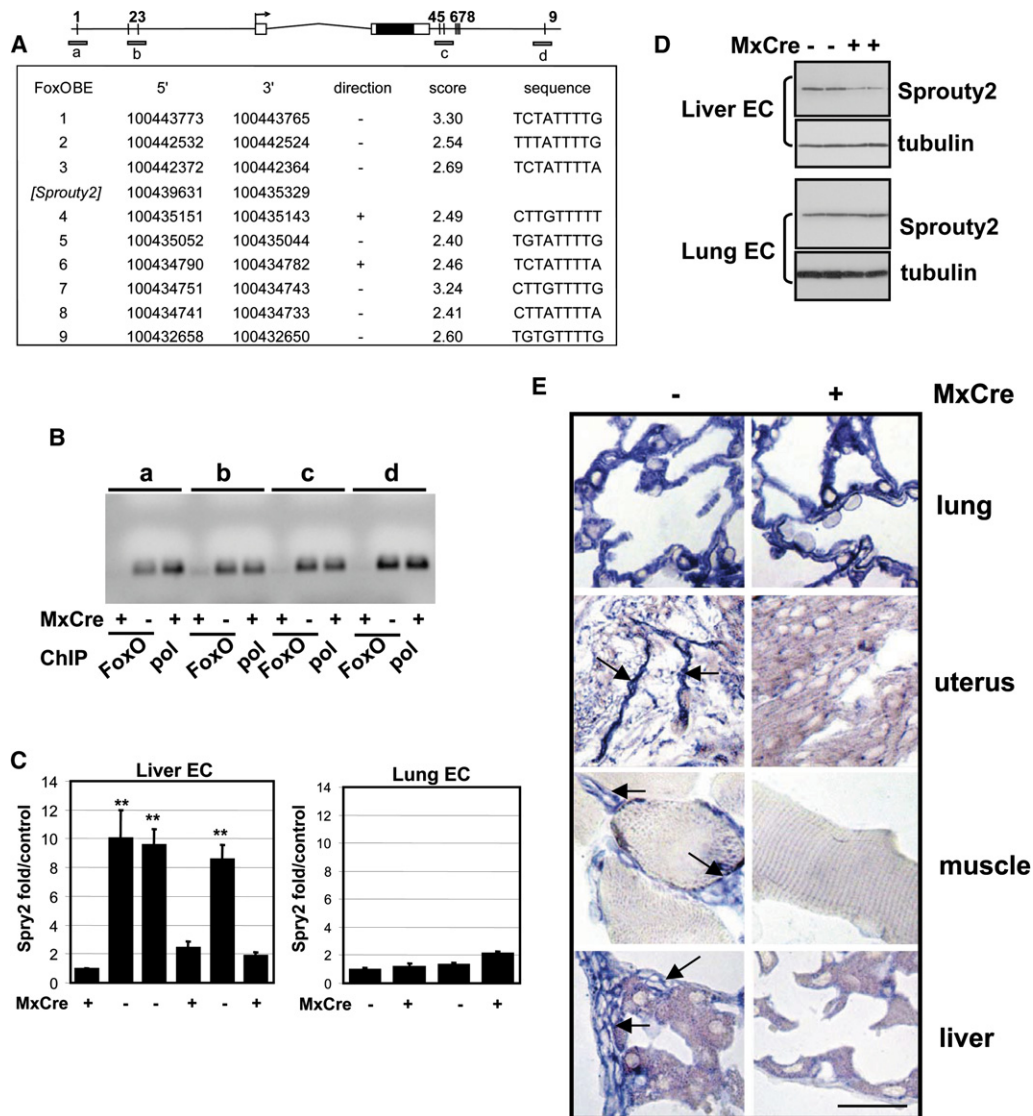


Figure 4. Regulation of Sprout2 Expression in Liver ECs by FoxOs

(A) Multiple conserved FoxO binding sites (predicted) in vicinity of *Sprout2* gene; ~11 kb of the genomic region is shown. Five of ten sites were conserved in >3 species including human and mouse (Supplemental Data). Sites were scored by 10-based logarithm of the likelihood ratio between the FoxO and background models.

(B) The FoxO BE occupancy by FoxOs. Soluble chromatin was prepared from *Mx-Cre*⁻ and *Mx-Cre*⁺ liver ECs and immunoprecipitated with a mixture of antibodies against the three FoxOs. Anti-pol II and anti-FoxO immunoprecipitated DNA (FoxO) was amplified, giving rise to ~110 bp products ([A–D], illustrated in A).

(C) Quantitative RT-PCR analysis for Sprout2. Expression of Sprout2 is tightly correlated with FoxO deletion (*Mx-Cre*⁺) in liver ECs, but not in lung ECs (**p < 0.01). Error bars = SE.

(D) Immunoblot analysis for Sprout2. Expression of Sprout2 is lower in FoxO deletion (*Mx-Cre*⁺) in liver ECs, but not in lung ECs, compared with control ECs. Duplicate loading shown for each EC line.

(E) RNA in situ hybridization using antisense Sprout2 probe tissues from *Mx-Cre*⁻ and *Mx-Cre*⁺ mice 3 weeks after pl-pC injection. Arrows point to EC with strong Sprout2 expression. Scale bar, 20 μ m.

To assess additional contributions from other validated or putative direct FoxO targets listed in Table 1, knock-down studies were conducted on an additional set of FoxO-upregulated genes (ADM, CTGF, MRC1, and CCRN4L) and FoxO-downregulated genes (PBX1, ID1,

and BMPER). These assays revealed that PBX1 exhibited robust activities in both EC proliferation and apoptosis assays similar to Sprout2, and two targets (CTGF and ADM) showed modest effects on EC growth but not on apoptosis (Figure S13). Taking into account the technical caveat

of insufficient knockdown, these functional data suggest that an additional but limited number of direct FoxO targets participate in control of EC homeostasis as well.

DISCUSSION

In this study, systematic genetic analysis provided formal proof that the FoxOs are tumor suppressors *in vivo*, albeit with a narrower tumor spectrum than might have been predicted from previous biochemical models but in line with inherited genetic syndromes targeting the PI3K pathway in humans. By demonstrating regulation of distinct sets of putative direct targets by FoxOs in thymocytes and ECs, this study also offers molecular insights into the highly tissue-restricted and lineage-specific actions of FoxO *in vivo*.

FoxO Transcription Factors Are Functionally Redundant in Tumor Suppression

The requirement for complete deletion of all three FoxO loci in lymphomas, despite mosaic deletion patterns in premalignant thymocytes, combined with the lack of an increased lymphoma incidence in *Mx-Cre*⁺ animals bearing any two floxed alleles, strongly argues for extensive functional redundancy with strong selective pressure for inactivation of all three FoxOs on the level of tumor formation. With regard to the molecular basis of lymphomagenesis in the setting of FoxO deficiency, our *in vitro* studies suggest that increased cell cycle progression, as well as resistance to proapoptotic stimuli, account for the increased incidence of lymphomas *in vivo*. Consistent with this interpretation, p27^{KIP1}, a known T cell lymphoma suppressor gene (Geisen et al., 2003; Kang-Decker et al., 2004; Martins and Berns, 2002) and FoxO target (Dijkers et al., 2000; Medema et al., 2000; Stahl et al., 2002), was identified as one of the most significantly downregulated genes with a high number of evolutionarily conserved BEs.

It is somewhat unanticipated that the tumor spectrum following deletion of the three FoxOs is so restricted given that misregulation of the PTEN/AKT axis results in a wide range of tumors, including carcinomas (skin, colon, prostate, etc.), which were not observed following deletion of the three FoxOs. It is unlikely that this relates to insufficient *Mx-Cre* activity in epithelial tissue compartments given our documentation of efficient Cre-mediated recombination by both PCR and strong reporter activation in a wide range of epithelial compartments, including skin, mammary tissue, and GI tract (Figure S8). Furthermore, deletion of the FoxOs using K14-Cre, which is strongly expressed in a wide range of epithelia, did not result in epithelial hyperplasia or cancer in animals that were permitted to age normally for up to 16 months of age (D.H.C. and George John, unpublished data). At the same time, we cannot exclude the possibility that a limited number of epithelial cell types may not be targeted efficiently by *Mx-Cre* and do in fact depend upon FoxO tumor suppression activity, or that certain epithelia require a longer latency than the lethal neoplasias observed in our model.

Such considerations gain relevance in light of FoxO1 deletions in a high percentage of human prostate cancers, although the existence of PI3K pathway mutations (e.g., PTEN) remains undetermined in those cancers with FoxO1 alterations (Dong et al., 2006). While the lack of neoplastic phenotypes in epithelial tissues does not diminish the importance of the FoxOs in other cell lineages, our genetic analysis strongly suggests that other signaling surrogates (presumably the mTOR-S6K arm) play more prominent roles in the cancer-relevant activities of the PI3K-AKT network in most epithelial compartments, consistent with the collective data from other labs (Neshat et al., 2001). In this regard, although relatively infrequent, lymphomas have been documented in human *PTEN*-germline syndromes, and alterations in the *PTEN* gene have been reported in spontaneous lymphoid neoplasms (Sakai et al., 1998). Moreover, mice with T cell-specific deletion of *Pten* uniformly develop T cell lymphomas (Suzuki et al., 2001).

In regard to the FoxO-deficient vascular phenotype, it is interesting that hemangiomas are characteristic of human disease syndromes resulting from germline *Pten* mutations such as Cowden's disease and Bannayan-Zonana syndrome (Wanner et al., 2001). Thus, the demonstration that FoxO inactivation is sufficient to drive development of hemangiomas suggests that misregulation of the FoxOs is a prime mechanism by which PTEN loss leads to hemangiomas in these patients. Along these lines, benign liver hemangiomas associated with TSC2 deficiency display nuclear FoxO due to inactivation of AKT pathway, whereas TSC2 deficiency in a *Pten*^{+/-} background leads to very aggressive lethal hemangiomas wherein FoxOs localize to the cytosol (Manning et al., 2005). Finally, such restricted cancer phenotypes following deletion of all three FoxOs reveals surprisingly tissue-specific roles for PTEN/AKT signaling surrogates in distinct lineages. These observations highlight the value of conducting *in vivo* genetic studies.

The FoxO Family Regulates Endothelial Cell Homeostasis

Hemangiomas occurred systemically but were most severe in the uterus, which is perhaps a consequence of the cyclic vascular remodeling that occurs in this organ (Heryanto and Rogers, 2002). Along similar lines, it is tempting to speculate that the hemangioma-susceptible nature of the liver and muscle, but not the pulmonary vasculature, may reflect the remodeling and regenerative capacity of these organ systems in the setting of injury (e.g., hepatectomy) or physiologic stress (e.g., exercise). Much less severe lesions were observed in *Mx-Cre*⁺;*FoxO1*^{L/L} mice but not in *FoxO3* or *FoxO4* nullizygous mice, arguing that FoxO1 is the most physiologically important regulator of endothelial stability. Nonetheless, successive inactivation of FoxO3 and/or FoxO4 in addition to FoxO1 resulted in hemangioma phenotypes of increasing severity, clearly indicating that both FoxO3 and FoxO4 also contribute to endothelial growth suppression *in vivo*.

Table 2. FoxO Targets in Thymocyte

	FoxO Target Genes	# of BE(s)	Conservation Score	# of 3-species BE(s)	CIS
Downregulated FoxO Target Genes	Npas3	10	29	6	
	Cdh8	10	31	4	
	Myef2	6	16	3	
	Cdkn1b	5	14	3	
	Dlgap1	10	29	2	Btl14
	Tmem25	8	23	2	
	Lrrtm3	7	20	2	
	Tbx4	5	14	2	
	Kcnj2	5	16	2	
	AJ430384	4	12	2	
	Efna5	4	12	2	
	Rest	8	22	1	
	Odz3	7	19	1	
	Dpf3	5	15	1	
	Bag5	5	13	1	
	Cacna1e	4	11	1	
	Olfm3	3	9	1	
	Gas7	3	9	1	
	Tmem71	3	9	1	
	Znrf4	3	8	1	
	Aqp7	2	6	1	
	C730036D15Rik	2	6	1	
	Kcnip4	2	6	1	
	Usp3	2	6	1	Evi98
	Myo1e	2	6	1	
	Tgfb2	2	6	1	
	Cdh23	2	6	1	
	Trem2	2	6	1	
	Klc3	1	3	1	
	Cryab	1	3	1	
	Cacna2d2	1	3	1	
	Ncbp2	1	3	1	
	Dmrt3	1	3	1	
Upregulated FoxO Target Genes	Sox5	25	71	6	Btl27
	Rora	14	39	4	
	Cacna2d1	13	37	3	
	Creb5	11	31	3	
	Igsf4d	11	32	3	
	Srgap3	10	29	3	
	Pfkfb2	7	19	3	

Table 2. Continued

FoxO Target Genes	# of BE(s)	Conservation Score	# of 3-species BE(s)	CIS
Pacs1	6	17	3	
Sox4	5	14	3	Evi16
Mmp16	11	33	2	
Slc12a1	9	25	2	
Dcamkl1	6	17	2	
4931406I20Rik	6	17	2	4931406I20Rik
Scn5a	5	15	2	
Sorl1	4	12	2	
Pou4f3	4	11	2	
Shox2	11	32	1	
Hoxd12	6	19	1	
Id4	6	17	1	
Hapln1	6	17	1	
Slc12a1	5	14	1	
Golph4	5	14	1	
Slc24a2	5	15	1	
Ppp1r9a	5	15	1	
Barx2	5	15	1	
Ddx47	4	11	1	
Abcd2	4	12	1	
Npy2r	3	9	1	
Shrm	3	8	1	
Igfbp3	3	8	1	
Flt1	2	6	1	
Dyx1c1	2	5	1	
D14Ert171e	2	5	1	

Sprouty2 Is a Major Direct Target of FoxO in Endothelial Cells

The rationale for emphasizing Sprouty2 for our in-depth biological validation studies rested on the high number of predicted FoxO DNA BEs, its known functions in branching morphogenesis, and its documented, albeit poorly understood, roles in growth inhibition. While Sprouty2 is not the sole mediator of the FoxO effects on EC growth and survival (see below), our studies prove that it is a major effector, as knockdown of Sprouty2 mimicked many of the phenotypic consequences of triple FoxO deletion. The FoxO-Sprouty2 link gains further appeal in light of previous work showing that the *Drosophila* Sprouty homolog functions as an antagonist of receptor tyrosine kinase (RTK) signaling pathways that regulate branching morphogenesis of airways (Hacohen et al., 1998; Kramer et al., 1999), a process with obvious parallels to vasculogenesis. Sprouty and its mammalian homologs (Sprouty1–4) are general inhibitors of RTK signaling

that function by dampening the RAS-RAF-MEK pathway (Gross et al., 2001; Reich et al., 1999). Finally, on a more speculative level, it was recently demonstrated that Sprouty2 protein contains iron-sulfur complexes and assembles into large 24 subunit particles that store electrical charge and thus could serve as intercellular redox sensors (Wu et al., 2005). Furthermore, Sprouty2 is subject to nitrosylation by nitric oxide (NO) (Wu et al., 2005), consistent with studies showing that forced expression of NO synthase phenocopies the Sprouty mutation in flies (Wingrove and O'Farrell, 1999). How these provocative findings relate to RTK inhibition remain to be determined, but the link between Sprouty proteins and NO is especially intriguing, given the importance of NO as a regulator of vascular endothelium and response to hypoxia, and given the fact that endothelium is a major site of NO synthesis. Thus, many lines of evidence support the view that Sprouty2 is a critical focal point for pathways relevant to vascular biology.

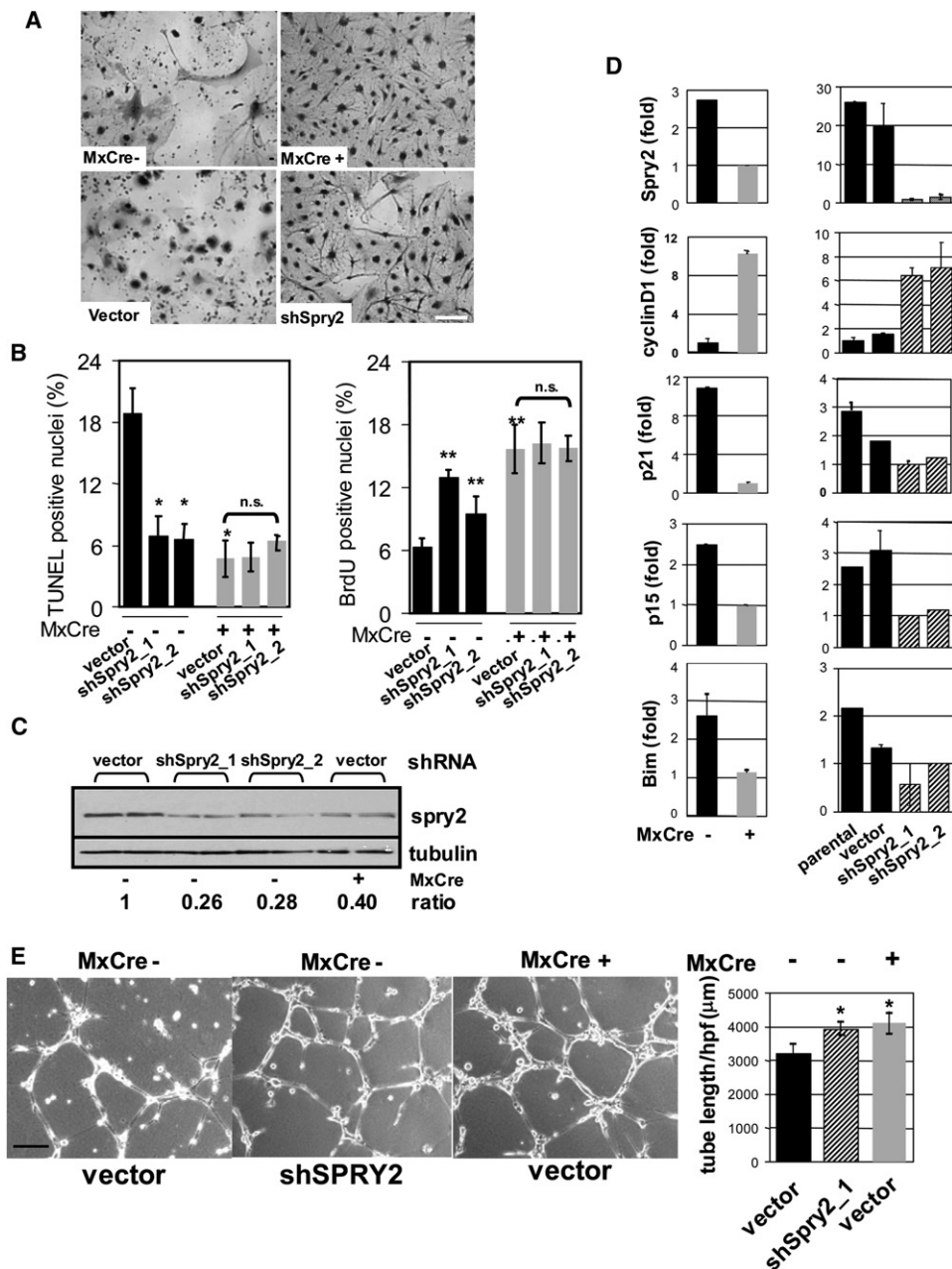


Figure 5. FoxOs Regulate Liver EC Angiogenic Response through Sprouty2

(A) Growth advantage of Mx-Cre⁺ over Mx-Cre⁻ liver ECs after 10 days culture. Sprouty2 knockdown in Mx-Cre⁻ liver ECs had a similar effect. Scale bar, 15 μ m.

(B) TUNEL and BrdU. Knockdown of Sprouty2 (shSpry2_1 and _2, shRNAs) in Mx-Cre⁻ liver ECs phenocopies cell growth and apoptosis phenotypes in Mx-Cre⁺ liver ECs; (*) indicates $p < 0.01$. Error bars = SE.

(C) Knockdown of endogenous Sprouty2 protein expression in Mx-Cre⁻ liver ECs by shSpry2. Two independent replicates are shown. Band densities were measured by ImageJ and normalized to tubulin. Ratio indicates normalized values over that of control (vector-infected Mx-Cre⁻ EC).

(D) Correlation of Sprouty2 expression with cyclinD1, p21, p15, and Bim level in liver ECs by quantitative RT-PCR. Knockdown of Sprouty2 with two different shRNAs (shSpry2_1 and _2) recapitulates above differences for cyclinD1, p21, p15, and Bim relative to parental untreated and vector-only controls (lower panels). Results shown are from triplicate experiments. Error bars = SE.

(E) VEGF-induced tube formation in liver ECs. Scale bar = 100 μ m. Average tubule length/hpf (\pm SD) measured by ImageJ software in multiple microscopic fields was plotted (* $p < 0.01$ versus vector-infected Mx-Cre⁻ EC).

At the same time, despite its potent negative regulatory effect on EC growth and survival, previous analysis of Sprouty2 knockout mice did not show high incidence of hemangioma (Taketomi et al., 2005; Shim et al., 2005). Absence of apparent hemangiomas in Sprouty2 knockout mice may therefore reflect that the FoxO null hemangioma phenotype may require the collaborative impact of additional FoxO target genes. Indeed, our functional analysis on an additional set of FoxO-target genes supports this view, pointing to important contributions of PBX1 in FoxO-regulated vascular biology in vivo (Figure S13).

In summary, by utilizing the in vivo system for somatic deletion of FoxO in multiple cell lineages, which resulted in clear phenotype-genotype correlations, and by employing computational prediction of FoxO BEs, we obtained evidence that the FoxOs effect unique biological consequences in different cell or tissue contexts via modulation of distinct downstream targets. These observations should motivate further analysis of FoxO targets for the development of novel points of therapeutic intervention in cancer and vascular disease but should also emphasize that the proper deployment of such therapies requires a systematic dissection of these targets in specific lineages and of the tissue contexts of these lineages.

EXPERIMENTAL PROCEDURES

Targeting Constructs, Generation, and Analysis of Mice

See Supplemental Data.

Immunohistochemistry and Immunofluorescence

Formalin-fixed, paraffin-embedded sections were used. For stains of pituitary tumors, sections were incubated with rabbit polyclonal antibodies to prolactin, GH, or ACTH (obtained through NHPP, NIDDK, and Dr. A.F. Parlow) followed by incubation with HRP-goat anti-rabbit IgG (Zymed) or with monoclonal antibodies to TSH, FSH, and LH (Lab-Vision/Neomarkers) utilizing the Histomouse-MAX kit (Zymed). In all cases, sections were then incubated with DAB and counterstained with hematoxylin. To visualize functional vasculature, we intravenously injected deeply anesthetized mice with 100 μ g FITC-labeled tomato lectin (Vector Laboratories) and perfused the hearts with 4% paraformaldehyde; tissues were then frozen in OCT medium. Images were acquired at a 0.5 μ m thickness interval using a Zeiss inverted microscope (Axiovert) with automated stage, and image deconvolution was carried out with the nearest neighbor algorithm.

Thymocyte Isolation, Proliferation, and Apoptosis

For analysis of thymocytes, fresh thymus was passed through a cell strainer (Becton Dickinson) in order to produce single cell suspensions for analysis, then resuspended in RPMI-1640 media containing 10% fetal calf serum. For thymocyte proliferation assays, cells were seeded in 96-well plates at 1×10^5 cells per well and subjected to the following conditions: no mitogen, PMA (1 ng/ml) + ionomycin (50 ng/ml), and 3 μ g/ml anti-CD3e (eBioscience) + 100 U IL-2. Cells were grown for 48 hr, and pulsed with 1 μ Ci [3H]-thymidine (Amersham) for the last 16 hr. Incorporated [3H]-thymidine was measured using the 1450 MicroBeta Trilux Scintillation and Luminescence Counter. For analysis of apoptosis, thymocytes were plated in 12-well plates (1×10^6 cells per well) and treated with 5 Gy γ -irradiation or 1 μ M dexamethasone for 18 hr. Cell viability was determined by staining the cells with propidium iodide and performing flow cytometric analysis.

Flow Cytometric Analysis

Single cell suspensions of thymus or EC were incubated with the following monoclonal antibodies: anti-CD4 (PE- or FITC-conjugated), anti-CD8 (PE- or APC-conjugated), anti-Mac-1-FITC, anti-CD3-PE, anti-CD25-APC, anti-CD44-PE, anti-Gr-1-PE, anti-CD19-APC, and anti-CD31-FITC (all from PharMingen). Flow cytometry analysis was performed on freshly stained samples.

Isolation and Characterization of Endothelial Cells, Microarray Analysis, and FoxO DNA Binding Element Studies

See Supplemental Data.

Quantitative RT-PCR Analysis

RNA was harvested using Trizol (Invitrogen) and the RNeasy kit (Qiagen). RNA was treated with RQ1 RNase-freeDNase (Promega), and cDNA was prepared utilizing Superscript II RNase H-Reverse transcriptase (Invitrogen). Quantitative RT-PCR was performed on cDNA samples utilizing the Quantitect SYBR Green PCR kit (Qiagen) and was run on the Stratagene Mx3000P. Primer sequences are available upon request.

Western Blot Analysis

Tissues and cells were lysed with RIPA buffer (20 mM Tris [pH 7.5], 150 mM NaCl, 1% Nonidet P-40, 0.5% Sodium Deoxycholate, 1 mM EDTA, 0.1% SDS) containing complete mini protease inhibitors (Roche). Western blots were performed utilizing 50 μ g of lysate protein, incubated with the following antibodies: anti-FKHR(FoxO1)/AFX (FoxO4) (Cell Signaling Technology) and anti-FKHL1(FoxO3) (Upstate Biotechnology).

Supplemental Data

The Supplemental Data for this article can be found online at <http://www.cell.com/cgi/content/full/128/2/309/DC1/>.

ACKNOWLEDGMENTS

We are grateful to Sarah Weiler and Mychelle Neptune for the generation of the conditional FoxO knockout mouse strains. We are also grateful to Karen Marmon, Alice Yu, and Yan Zhang for their assistance in the animal facility. We thank Nabeel El-Bardeesy, Susan Dymecki, Klaus Rajewsky, A.F. Parlow, the NCI BRB Preclinical Repository for reagents, and the DFCI-Broad RNAi Consortium for lentiviral shRNA vectors. We also thank Dong-In Yuk for assistance with RISH. D.G.G. is an Investigator of the Howard Hughes Medical Institute. J.-H.P. and Z.D. are Damon Runyon Fellows supported by the Damon Runyon Cancer Research Foundation. D.H.C. is a Sidney Kimmel Foundation Scholar and supported by the Mary Kay Ash and Lance Armstrong Foundations. This work was supported by grants to D.H.C., D.G.G., L.C., W.H.W., and R.A.D. from the NIH. R.A.D. is an American Cancer Society Research Professor and an Ellison Medical Foundation Scholar and supported by the Robert A. and Renee E. Belfer Foundation Institute for Innovative Cancer Science.

Received: June 5, 2006

Revised: October 16, 2006

Accepted: December 26, 2006

Published: January 25, 2007

REFERENCES

- Anderson, M.J., Viars, C.S., Czekay, S., Cavenee, W.K., and Arden, K.C. (1998). Cloning and characterization of three human forkhead genes that comprise an FKHR-like gene subfamily. *Genomics* 47, 187–199.
- Benezra, R. (2001). Role of Id proteins in embryonic and tumor angiogenesis. *Trends Cardiovasc. Med.* 11, 237–241.

- Biggs, W.H., 3rd, Cavennee, W.K., and Arden, K.C. (2001). Identification and characterization of members of the FKHR (FOX O) subclass of winged-helix transcription factors in the mouse. *Mamm. Genome* 12, 416–425.
- Bikfalvi, A., Klein, S., Pintucci, G., and Rifkin, D.B. (1997). Biological roles of fibroblast growth factor-2. *Endocr. Rev.* 18, 26–45.
- Brunet, A., Bonni, A., Zigmond, M.J., Lin, M.Z., Juo, P., Hu, L.S., Anderson, M.J., Arden, K.C., Blenis, J., and Greenberg, M.E. (1999). Akt promotes cell survival by phosphorylating and inhibiting a Forkhead transcription factor. *Cell* 96, 857–868.
- Castrillon, D.H., Miao, L., Kollipara, R., Horner, J.W., and DePinho, R.A. (2003). Suppression of ovarian follicle activation in mice by the transcription factor Foxo3a. *Science* 301, 215–218.
- Cook-Mills, J.M. (2002). VCAM-1 signals during lymphocyte migration: role of reactive oxygen species. *Mol. Immunol.* 39, 499–508.
- Cross, D.A., Alessi, D.R., Cohen, P., Andjelkovich, M., and Hemmings, B.A. (1995). Inhibition of glycogen synthase kinase-3 by insulin mediated by protein kinase B. *Nature* 378, 785–789.
- Cully, M., You, H., Levine, A.J., and Mak, T.W. (2006). Beyond PTEN mutations: the PI3K pathway as an integrator of multiple inputs during tumorigenesis. *Nat. Rev. Cancer* 6, 184–192.
- Di Cristofano, A., Pesce, B., Cordon-Cardo, C., and Pandolfi, P.P. (1998). Pten is essential for embryonic development and tumour suppression. *Nat. Genet.* 19, 348–355.
- Dijkers, P.F., Medema, R.H., Pals, C., Banerji, L., Thomas, N.S., Lam, E.W., Burgering, B.M., Raaijmakers, J.A., Lammers, J.W., Koenderman, L., et al. (2000). Forkhead transcription factor FKHR-L1 modulates cytokine-dependent transcriptional regulation of p27(KIP1). *Mol. Cell. Biol.* 20, 9138–9148.
- Dong, X.Y., Chen, C., Sun, X., Guo, P., Vessella, R.L., Wang, R.X., Chung, L.W., Zhou, W., and Dong, J.T. (2006). FOXO1A is a candidate for the 13q14 tumor suppressor gene inhibiting androgen receptor signaling in prostate cancer. *Cancer Res.* 66, 6998–7006.
- Ferrara, N., Gerber, H.P., and LeCouter, J. (2003). The biology of VEGF and its receptors. *Nat. Med.* 9, 669–676.
- Flores, E.R., Tsai, K.Y., Crowley, D., Sengupta, S., Yang, A., McKeon, F., and Jacks, T. (2002). p63 and p73 are required for p53-dependent apoptosis in response to DNA damage. *Nature* 416, 560–564.
- Flores, E.R., Sengupta, S., Miller, J.B., Newman, J.J., Bronson, R., Crowley, D., Yang, A., McKeon, F., and Jacks, T. (2005). Tumor predisposition in mice mutant for p63 and p73: evidence for broader tumor suppressor functions for the p53 family. *Cancer Cell* 7, 363–373.
- Freeman, D., Lesche, R., Kertesz, N., Wang, S., Li, G., Gao, J., Groszer, M., Martinez-Diaz, H., Rozengurt, N., Thomas, G., et al. (2006). Genetic background controls tumor development in PTEN-deficient mice. *Cancer Res.* 66, 6492–6496.
- Furuyama, T., Nakazawa, T., Nakano, I., and Mori, N. (2000). Identification of the differential distribution patterns of mRNAs and consensus binding sequences for mouse DAF-16 homologues. *Biochem. J.* 349, 629–634.
- Furuyama, T., Kitayama, K., Shimoda, Y., Ogawa, M., Sone, K., Yoshida-Araki, K., Hisatsune, H., Nishikawa, S., Nakayama, K., Ikeda, K., et al. (2004). Abnormal angiogenesis in Foxo1 (Fkhr)-deficient mice. *J. Biol. Chem.* 279, 34741–34749.
- Geisen, C., Karsunky, H., Yucel, R., and Moroy, T. (2003). Loss of p27(Kip1) cooperates with cyclin E in T-cell lymphomagenesis. *Oncogene* 22, 1724–1729.
- Goumans, M.J., Lebrin, F., and Valdimarsdottir, G. (2003). Controlling the angiogenic switch: a balance between two distinct TGF- β receptor signaling pathways. *Trends Cardiovasc. Med.* 13, 301–307.
- Gross, I., Bassit, B., Benezra, M., and Licht, J.D. (2001). Mammalian sprouty proteins inhibit cell growth and differentiation by preventing ras activation. *J. Biol. Chem.* 276, 46460–46468.
- Hacohen, N., Kramer, S., Sutherland, D., Hiromi, Y., and Krasnow, M.A. (1998). Sprouty encodes a novel antagonist of FGF signaling that patterns apical branching of the Drosophila airways. *Cell* 92, 253–263.
- Hay, N. (2005). The Akt-mTOR tango and its relevance to cancer. *Cancer Cell* 8, 179–183.
- Hayashi, M., Kim, S.W., Imanaka-Yoshida, K., Yoshida, T., Abel, E.D., Eliceiri, B., Yang, Y., Ulevitch, R.J., and Lee, J.D. (2004). Targeted deletion of BMK1/ERK5 in adult mice perturbs vascular integrity and leads to endothelial failure. *J. Clin. Invest.* 113, 1138–1148.
- Heryanto, B., and Rogers, P.A. (2002). Regulation of endometrial endothelial cell proliferation by oestrogen and progesterone in the ovariectomized mouse. *Reproduction* 123, 107–113.
- Hosaka, T., Biggs, W.H., 3rd, Tieu, D., Boyer, A.D., Varki, N.M., Cavennee, W.K., and Arden, K.C. (2004). Disruption of forkhead transcription factor (FOXO) family members in mice reveals their functional diversification. *Proc. Natl. Acad. Sci. USA* 101, 2975–2980.
- Inoki, K., Li, Y., Zhu, T., Wu, J., and Guan, K.L. (2002). TSC2 is phosphorylated and inhibited by Akt and suppresses mTOR signalling. *Nat. Cell Biol.* 4, 648–657.
- Jacobs, F.M., van der Heide, L.P., Wijchers, P.J., Burbach, J.P., Hoekman, M.F., and Smidt, M.P. (2003). FoxO6, a novel member of the FoxO class of transcription factors with distinct shuttling dynamics. *J. Biol. Chem.* 278, 35959–35967.
- Junger, M.A., Rintelen, F., Stocker, H., Wasserman, J.D., Vegh, M., Radimerski, T., Greenberg, M.E., and Hafen, E. (2003). The Drosophila forkhead transcription factor FOXO mediates the reduction in cell number associated with reduced insulin signaling. *J. Biol.* 2, 20.
- Kang-Decker, N., Tong, C., Boussouar, F., Baker, D.J., Xu, W., Leontovich, A.A., Taylor, W.R., Brindle, P.K., and van Deursen, J.M. (2004). Loss of CBP causes T cell lymphomagenesis in synergy with p27Kip1 insufficiency. *Cancer Cell* 5, 177–189.
- Kato, J., Tsuruda, T., Kita, T., Kitamura, K., and Eto, T. (2005). Adrenomedullin: a protective factor for blood vessels. *Arterioscler. Thromb. Vasc. Biol.* 25, 2480–2487.
- Kramer, S., Okabe, M., Hacohen, N., Krasnow, M.A., and Hiromi, Y. (1999). Sprouty: a common antagonist of FGF and EGF signaling pathways in Drosophila. *Development* 126, 2515–2525.
- Kuhn, R., Schwenk, F., Aguet, M., and Rajewsky, K. (1995). Inducible gene targeting in mice. *Science* 269, 1427–1429.
- Le Jan, S., Amy, C., Cazes, A., Monnot, C., Lamande, N., Favier, J., Philippe, J., Sibony, M., Gasc, J.M., Corvol, P., et al. (2003). Angiopoietin-like 4 is a proangiogenic factor produced during ischemia and in conventional renal cell carcinoma. *Am. J. Pathol.* 162, 1521–1528.
- Lee, M.H., Williams, B.O., Mulligan, G., Mukai, S., Bronson, R.T., Dyson, N., Harlow, E., and Jacks, T. (1996). Targeted disruption of p107: functional overlap between p107 and Rb. *Genes Dev.* 10, 1621–1632.
- Li, G., Robinson, G.W., Lesche, R., Martinez-Diaz, H., Jiang, Z., Rozengurt, N., Wagner, K.U., Wu, D.C., Lane, T.F., Liu, X., et al. (2002). Conditional loss of PTEN leads to precocious development and neoplasia in the mammary gland. *Development* 129, 4159–4170.
- Lin, L., Hron, J.D., and Peng, S.L. (2004). Regulation of NF- κ B, Th activation, and autoinflammation by the forkhead transcription factor Foxo3a. *Immunity* 21, 203–213.
- Martins, C.P., and Berns, A. (2002). Loss of p27(Kip1) but not p21(Cip1) decreases survival and synergizes with MYC in murine lymphomagenesis. *EMBO J.* 21, 3739–3748.
- Manning, B.D., Logsdon, N.M., Lipovsky, A.I., Abbott, D., Kwiatkowski, D.J., and Cantley, L.C. (2005). Feedback inhibition of Akt signalling limits the growth of tumors lacking Tsc2. *Genes Dev.* 19, 1773–1778.

- Medema, R.H., Kops, G.J., Bos, J.L., and Burgering, B.M. (2000). AFX-like Forkhead transcription factors mediate cell-cycle regulation by Ras and PKB through p27kip1. *Nature* 404, 782–787.
- Mouta Carreira, C., Nasser, S.M., di Tomaso, E., Padera, T.P., Boucher, Y., Tomarev, S.I., and Jain, R.K. (2001). LYVE-1 is not restricted to the lymph vessels: expression in normal liver blood sinusoids and down-regulation in human liver cancer and cirrhosis. *Cancer Res.* 61, 8079–8084.
- Neshat, M.S., Mellingerhoff, I.K., Tran, C., Stiles, B., Thomas, G., Petersen, R., Frost, P., Gibbons, J.J., Wu, H., and Sawyers, C.L. (2001). Enhanced sensitivity of PTEN-deficient tumors to inhibition of FRAP/mTOR. *Proc. Natl. Acad. Sci. USA* 98, 10314–10319.
- Nikitenko, L.L., Fox, S.B., Kehoe, S., Rees, M.C., and Bicknell, R. (2006). Adrenomedullin and tumour angiogenesis. *Br. J. Cancer* 94, 1–7.
- Podsypanina, K., Ellenson, L.H., Nemes, A., Gu, J., Tamura, M., Yamada, K.M., Cordon-Cardo, C., Cattoretti, G., Fisher, P.E., and Parsons, R. (1999). Mutation of Pten/Mmac1 in mice causes neoplasia in multiple organ systems. *Proc. Natl. Acad. Sci. USA* 96, 1563–1568.
- Potente, M., Urbich, C., Sasaki, K.I., Hofmann, W.K., Heeschen, C., Aicher, A., Kolipara, R., Depinho, R.A., Zeiher, A.M., and Dimmeler, S. (2005). Involvement of Foxo transcription factors in angiogenesis and postnatal neovascularization. *J. Clin. Invest.* 115, 2382–2392.
- Puig, O., Marr, M.T., Ruhf, M.L., and Tjian, R. (2003). Control of cell number by Drosophila FOXO: downstream and feedback regulation of the insulin receptor pathway. *Genes Dev.* 17, 2006–2020.
- Ramirez, F., Pereira, L., Zhang, H., and Lee, B. (1993). The fibrillin-Marfan syndrome connection. *Bioessays* 15, 589–594.
- Reich, A., Sapir, A., and Shilo, B. (1999). Sprouty is a general inhibitor of receptor tyrosine kinase signaling. *Development* 126, 4139–4147.
- Sage, J., Mulligan, G.J., Attardi, L.D., Miller, A., Chen, S., Williams, B., Theodorou, E., and Jacks, T. (2000). Targeted disruption of the three Rb-related genes leads to loss of G(1) control and immortalization. *Genes Dev.* 14, 3037–3050.
- Sakai, A., Thieblemont, C., Wellmann, A., Jaffe, E.S., and Raffeld, M. (1998). PTEN gene alterations in lymphoid neoplasms. *Blood* 92, 3410–3415.
- Schneider, A., Zhang, Y., Guan, Y., Davis, L.S., and Breyer, M.D. (2003). Differential, inducible gene targeting in renal epithelia, vascular endothelium, and viscera of Mx1Cre mice. *Am. J. Physiol. Renal Physiol.* 284, F411–F417.
- Seoane, J., Le, H.V., Shen, L., Anderson, S.A., and Massague, J. (2004). Integration of Smad and forkhead pathways in the control of neuroepithelial and glioblastoma cell proliferation. *Cell* 117, 211–223.
- Shim, K., Minowada, G., Coling, D.E., and Martin, G.R. (2005). Sprouty2, a mouse deafness gene, regulates cell fate decisions in the auditory sensory epithelium by antagonizing FGF signaling. *Dev. Cell.* 8, 553–564.
- Shiojima, I., and Walsh, K. (2002). Role of Akt signaling in vascular homeostasis and angiogenesis. *Circ. Res.* 90, 1243–1250.
- Skurk, C., Maatz, H., Kim, H.S., Yang, J., Abid, M.R., Aird, W.C., and Walsh, K. (2004). The Akt-regulated forkhead transcription factor FOXO3a controls endothelial cell viability through modulation of the caspase-8 inhibitor FLIP. *J. Biol. Chem.* 279, 1513–1525.
- Stahl, M., Dijkers, P.F., Kops, G.J., Lens, S.M., Coffey, P.J., Burgering, B.M., and Medema, R.H. (2002). The forkhead transcription factor FoxO regulates transcription of p27Kip1 and Bim in response to IL-2. *J. Immunol.* 168, 5024–5031.
- Suzuki, A., Yamaguchi, M.T., Ohteki, T., Sasaki, T., Kaisho, T., Kimura, Y., Yoshida, R., Wakeham, A., Higuchi, T., Fukumoto, M., et al. (2001). T cell-specific loss of Pten leads to defects in central and peripheral tolerance. *Immunity* 14, 523–534.
- Taketomi, T., Yoshiga, D., Taniguchi, K., Kobayashi, T., Nonami, A., Kato, R., Sasaki, M., Sasaki, A., Ishibashi, H., Moriyama, M., et al. (2005). Loss of mammalian Sprouty2 leads to enteric neuronal hyperplasia and esophageal achalasia. *Nat. Neurosci.* 8, 855–857.
- van der Heide, L.P., Jacobs, F.M., Burbach, J.P., Hoekman, M.M., and Smidt, M.P. (2005). FoxO6 transcriptional activity is regulated by Thr26 and Ser184, independent of nucleo-cytoplasmic shuttling. *Biochem. J.* 391, 623–629.
- Wang, S., Gao, J., Lei, Q., Rozengurt, N., Pritchard, C., Jiao, J., Thomas, G.V., Li, G., Roy-Burman, P., Nelson, P.S., et al. (2003). Prostate-specific deletion of the murine Pten tumor suppressor gene leads to metastatic prostate cancer. *Cancer Cell* 4, 209–221.
- Wanner, M., Celebi, J.T., and Peacocke, M. (2001). Identification of a PTEN mutation in a family with Cowden syndrome and Bannayan-Zonana syndrome. *J. Am. Acad. Dermatol.* 44, 183–187.
- Wingrove, J.A., and O'Farrell, P.H. (1999). Nitric oxide contributes to behavioral, cellular, and developmental responses to low oxygen in Drosophila. *Cell* 98, 105–114.
- Wu, X., Alexander, P.B., He, Y., Kikkawa, M., Vogel, P.D., and McKnight, S.L. (2005). Mammalian sprouty proteins assemble into large monodisperse particles having the properties of intracellular nanobatteries. *Proc. Natl. Acad. Sci. USA* 102, 14058–14062.
- You, M.J., Castrillon, D.H., Bastian, B.C., O'Hagan, R.C., Bosenberg, M.W., Parsons, R., Chin, L., and Depinho, R.A. (2002). Genetic analysis of Pten and Ink4a/Arf interactions in the suppression of tumorigenesis in mice. *Proc. Natl. Acad. Sci. USA* 99, 1455–1460.